Acta Cryst. (1981). B37, 50–56

Compounds with Intermediate Spin. 5. X-ray Study of Tris(*N*,*N*-dimethyldithiocarbamato)iron(III) at the Two Extreme Temperatures 25 and 400 K

BY J. ALBERTSSON, Å. OSKARSSON, K. STÅHL, C. SVENSSON AND I. YMÉN

Inorganic Chemistry 1 *and* 2, *Chemical Center, University of Lund, POB* 740, *S*-220 07 *Lund* 7, *Sweden*

(*Received* 12 *May* 1980; *accepted* 18 *August* 1980)

Abstract

$Fe[S_2CN(CH_3)_2]_3$ has a temperature-dependent magnetic moment. Its crystal structure has been determined at 25 and 400 K from X-ray intensities collected with a diffractometer equipped with a Be-walled liquid He cryostat and a microfurnace. The space group is *Pbca* with $Z = 8$ at both temperatures: $a = 17{\cdot}288$ (50), $b = 19{\cdot}947$ (26), $c = 9{\cdot}998$ (13) Å at 25 K ($\mu_{eff} \simeq 2{\cdot}0$) and $a = 17{\cdot}6961$ (8), $b = 20{\cdot}7906$ (10), $c = 10{\cdot}1630$ (6) Å at 400 K ($\mu_{eff} = 4{\cdot}83$). The refinements converged to $R = 0{\cdot}046$ (25 K) and 0·058 (400 K). At both temperatures the mononuclear tris(dithiocarbamato) complexes with pseudosymmetry D_3 are van der Waals packed. The main structural difference between the low- and high-spin complexes is the Fe–S distances: the average length is 2·302 (3) at 25 and 2·415 (4) Å at 400 K. The 25 K low-spin complex is the least distorted. The average apparent decrease in bond lengths between non-H atoms in the planar ligands is only 0·011 (3) Å when the temperature rises from 25 to 400 K. Preliminary ESCA studies indicate a charge redistribution in the complex: the low-spin Fe–S bond is more covalent than the high-spin bond.

Introduction

Most complexes formed between Fe^{III} and substituted dithiocarbamate ligands have magnetic moments which are strongly temperature dependent (White, Roper, Kokot, Waterman & Martin, 1964; Ewald, Martin, Sinn & White, 1969). The present series of investigations (Albertsson, Elding & Oskarsson, 1979, and references therein) aims at correlating the magnetic behaviour of various $Fe(S_2CNR_2)_3$ complexes with the geometrical features of the complexes: (i) the size, symmetry and distortior of the FeS_6 core at different temperatures, (ii) bond distances and angles, and conformations of the ligand molecules, especially the S_2CNC_2 part, and (iii) the crystal packing of the complexes.

The simplest Fe^{III} dithiocarbamate is tris(*N*,*N*-dimethyldithiocarbamato)iron(III). Its crystal structure has previously been investigated at 150 ($\mu_{eff} = 2{\cdot}40$)* and 295 K ($\mu_{eff} = 4{\cdot}03$) (Albertsson & Oskarsson, 1977). A Be-walled liquid He cryostat has now been developed for single-crystal diffraction studies down to 20 K on our CAD-4 diffractometer (Albertsson, Oskarsson & Ståhl, 1979). We have also built a stable microfurnace similar to the one described by Lissalde, Abrahams & Bernstein (1978) for use in the interval 300–600 K. This equipment has been employed to determine the difference in size of Fe^{III} in the low- and high-spin states in a single compound, and how this difference (and the accompanying change in thermal motion of the atoms) affects the distortion and packing of the complex and the geometry of the ligands. Because of crystal decomposition above 400 K ($\mu_{eff} = 4{\cdot}83$) the pure high-spin state could only be reached by extrapolation. Since high-angle intensities are lacking, the present intensity-data set at 25 K does not warrant a determination of the charge density in the complex, but the result of a preliminary ESCA study is reported.

Experimental

Single crystals of $Fe[S_2CN(CH_3)_2]_3$ were prepared as described by Albertsson & Oskarsson (1977). Table 1 gives information concerning the crystal data, the collection and reduction of the intensity-data sets and the refinements based on them. The 25 K intensity-data set was collected from three different crystals with the liquid He cryostat. The experimental procedure used is described by Albertsson, Oskarsson & Ståhl (1979). Since the κ motion of the CAD-4 goniostat is limited to $\pm 60°$ by the liquid He transfer line and the goniometer head, the three crystals were mounted in different orientations: Nos. 1 and 2 on glass fibres and No. 3 in

* μ_{eff} is the number of Bohr magnetons (1 Bohr magneton $\simeq 9{\cdot}274 \times 10^{-24}$ J T^{-1}).

0567-7408/81/010050-07$01.00

Table 1. *Crystal data, collection and reduction of intensities, and the least-squares refinement of* $Fe[S_2CN(CH_3)_2]_3$

$M_r(C_9H_{18}FeN_3S_6) = 416{\cdot}47$, space group: *Pbca*, $Z = 8$. At 25 K (crystals No. 1, 2, 3) $a = 17{\cdot}288\ (50)$, $b = 19{\cdot}947\ (26)$, $c = 9{\cdot}998\ (13)$ Å, $V = 3348\ (30)$ Å^3, $D_x = 1{\cdot}604$ Mg m^{-3}. At 400 K (crystal No. 4) $a = 17{\cdot}6961\ (8)$, $b = 20{\cdot}7906\ (10)$, $c = 10{\cdot}1630\ (6)$ Å, $V = 3739\ (6)$ Å^3, $D_x = 1{\cdot}480$ Mg m^{-3}.

Crystal No.	1	2	3	4
Crystal size (mm)	0·06 × 0·28 × 0·36	0·12 × 0·25 × 0·32	0·06 × 0·32 × 0·30	0·12 × 0·25 × 0·32
Radiation	Cu $K\alpha$	Cu $K\alpha$	Mo $K\alpha$	Cu $K\alpha$
Max. sin θ/λ (Å^{-1})	0·46	0·46	1·01	0·61
Scan type	ω	ω	ω	ω–2θ
Scan width, $\Delta\omega$ (°)	1·0 + 0·3 tan θ	1·0 + 0·3 tan θ	0·8 + 0·5 tan θ	0·7 + 0·5 tan θ
$\sigma_c(I)/I$ requested in a scan	0·030	0·030	0·025	0·020
Max. recording time (s)	120	120	120	180
μ (mm^{-1})	13·52	13·52	1·52	12·51
Range of transmission factor*	0·08–0·36	0·05–0·23	0·74–0·91	0·08–0·32
Number of reflexions recorded	1126	615	708	3979
Number of reflexions in final LS cycles, m	700	380	657	1295
Number of parameters refined, n	229	229	229	173
$R = \sum \lvert\Delta F\rvert / \sum \lvert F_o\rvert$†	0·059	0·029	0·042	0·058
overall value		0·046		–
$R_w = [\sum w(\Delta F)^2 / \sum w\lvert F_o\rvert^2]^{1/2}$	0·074	0·040	0·054	0·065
overall value		0·061		–
$S = [\sum w(\Delta F)^2/(m-n)]^{1/2}$		1·098		1·070
C_1 (weighting function)		0·050		0·045
C_2 (weighting function)		1·50		–
$g \times 10^{-4}$ (extinction)		–		0·24 (6)

* Refers to the absorption in the crystal. The 25 K data were also corrected for absorption in the Be walls of the liquid He cryostat.
† $\Delta F = \lvert F_o\rvert - \lvert F_c\rvert$.

an open, thin-walled capillary made of Lindemann glass. For all three crystals the temperature was in the range 22–28 K during the experiment. Due to mishaps with the electronic temperature controller the temperature variation sometimes increased to more than ±2 K about the mean, *i.e.* the usually attainable stability. There are some systematic errors in the structural parameters which are probably caused by the temperature variation, but these errors must be small. At 25 K the zero-point intramolecular movements predominate over all thermal effects in compounds of this type. In order to exclude weak reflexions from the measurements on crystal No. 3, all intensities in the sin θ/λ range 0·46–1·01 Å^{-1} were calculated with a model based on the data for crystals Nos. 1 and 2.

Crystal No. 4 (Table 1) was mounted in the microfurnace shown in Fig. 1. To improve the stability and allow water cooling to be introduced between the furnace and the φ-axis shaft of the goniostat, the furnace is mounted on the same type of x,y,z adjustments as is used on the liquid He cryostat. The crystal was secured with 'Superepoxy' cement on a glass fibre. The regulating Pt/Pt (10% Rh) thermocouple was positioned less than 1 mm below the crystal. The temperature was 400 K, with a long-term stability better than ±1 K.

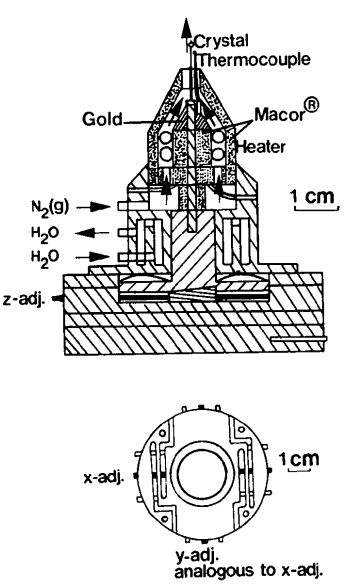

Fig. 1. Stable, water-cooled microfurnace for CAD-4. The heater section is analogous to that of Lissalde, Abrahams & Bernstein (1978). The base with x,y,z translation adjustments is of the same type as used with the liquid He cryostat.

During data collection, standard reflexions were checked at regular intervals. No systematic variation in their intensities or in the orientation of the crystals was

Table 2. *Positional parameters* ($\times 10^5$, *for* H $\times 10^3$) *and approximate isotropic thermal parameters of* $Fe[S_2CN(CH_3)_2]_3$ *at* 25 *and* 400 K, *with e.s.d.'s*

	25 K				400 K			
	x	*y*	*z*	*B* (Å²)	*x*	*y*	*z*	*B* (Å²)
Fe	56236 (6)	12194 (5)	34756 (13)	0·6 (1)	56447 (8)	12217 (7)	33422 (16)	4·8 (1)
S(1)	47242 (10)	7918 (8)	20197 (21)	1·1 (1)	46911 (16)	8295 (14)	18564 (31)	6·7 (1)
S(2)	48129 (10)	21144 (8)	30354 (21)	1·1 (1)	48269 (17)	21194 (13)	28218 (36)	7·3 (1)
N(1)	37545 (33)	17616 (30)	12090 (73)	1·2 (2)	37871 (52)	17739 (58)	10804 (112)	7·8 (4)
C(1)	43337 (37)	15865 (31)	19637 (84)	0·9 (2)	43577 (55)	16035 (55)	18113 (113)	6·3 (4)
C(2)	33647 (48)	12975 (39)	2909 (99)	1·5 (2)	33894 (76)	13299 (89)	2272 (158)	11·5 (7)
C(3)	34520 (52)	24488 (40)	12203 (100)	1·6 (2)	35100 (79)	24144 (90)	10275 (172)	12·7 (7)
S(3)	64018 (9)	2883 (8)	32302 (20)	1·0 (1)	64273 (15)	2843 (12)	30128 (29)	6·0 (1)
S(4)	65396 (10)	15395 (8)	19229 (20)	1·0 (1)	66202 (15)	15243 (12)	17777 (28)	5·6 (1)
N(2)	75900 (31)	5636 (27)	15696 (65)	0·8 (2)	75944 (46)	5679 (37)	14520 (86)	5·4 (3)
C(4)	69455 (35)	7580 (31)	21473 (80)	0·8 (2)	69622 (51)	7540 (45)	19976 (96)	4·9 (3)
C(5)	79022 (50)	−1116 (42)	17797 (113)	1·6 (2)	78810 (63)	−807 (57)	16498 (121)	7·8 (4)
C(6)	80287 (42)	9965 (40)	6706 (101)	1·2 (2)	80383 (60)	9771 (59)	6127 (123)	7·5 (4)
S(5)	62930 (10)	17471 (8)	51524 (20)	0·9 (1)	63151 (14)	17464 (12)	50959 (28)	5·5 (1)
S(6)	50515 (10)	8360 (8)	54122 (21)	1·0 (1)	50870 (14)	8478 (13)	53752 (27)	6·1 (1)
N(3)	57781 (35)	13550 (27)	75805 (74)	1·0 (2)	58161 (52)	13595 (36)	73982 (95)	5·3 (3)
C(7)	57112 (36)	13251 (31)	62591 (94)	1·1 (2)	57397 (53)	13282 (42)	61256 (102)	4·4 (3)
C(8)	52488 (47)	10198 (41)	84833 (90)	1·2 (2)	53066 (84)	10151 (60)	82875 (120)	8·9 (5)
C(9)	64038 (44)	17369 (39)	82006 (92)	1·1 (2)	64088 (81)	17210 (56)	80395 (113)	8·0 (4)

detected. For crystals Nos. 1 and 2 the intensities were calculated with the peak-location method (Lehmann & Larsen, 1974) to avoid errors in weak reflexions at low θ angles. Values of I and $\sigma_c(I)$ were corrected for Lorentz, polarization and absorption effects, the latter by numerical integration [$\sigma_c(I)$ is based on counting statistics].

At both temperatures the cell dimensions were obtained from θ values determined as $\theta_{hkl} = (\omega_{hkl} - \omega_{\bar{h}\bar{k}\bar{l}})/2$ with the CAD-4 diffractometer in the bisecting mode and measuring $\omega_{\bar{h}\bar{k}\bar{l}}$ at negative θ angles. The large ω motions of the standard CAD-4 procedure (DETTH) to measure θ angles prevent it from being used with the liquid He cryostat or the microfurnace. The cell dimensions at 25 and 400 K are based on 22 and 47 θ values, respectively, measured with Ni-filtered Cu $K\alpha$ radiation ($\lambda = 1{\cdot}54056$ Å).

The ESCA experiments were made on an AEI ES200 electron spectrometer by a procedure described elsewhere (Folkesson, 1973).

Table 2 (*cont.*)

B values for H atoms at 25 K are 1·5 Å², at 400 K 8·0 Å².

	25 K			400 K		
	x	*y*	*z*	*x*	*y*	*z*
H(1C2)	335 (5)	148 (4)	−56 (9)	340	142	−76
H(2C2)	277 (5)	123 (4)	53 (8)	284	123	46
H(3C2)	363 (4)	87 (4)	39 (9)	367	88	33
H(1C3)	340 (5)	259 (4)	216 (9)	344	260	201
H(2C3)	293 (5)	246 (4)	81 (8)	301	249	60
H(3C3)	381 (5)	272 (4)	93 (9)	387	275	64
H(1C5)	761 (5)	−38 (4)	190 (9)	751	−37	212
H(2C5)	821 (5)	−28 (4)	134 (9)	836	−7	227
H(3C5)	812 (5)	−10 (4)	267 (9)	804	−27	81
H(1C6)	859 (5)	92 (4)	63 (9)	843	125	106
H(2C6)	796 (4)	145 (4)	91 (9)	771	129	5
H(3C6)	787 (5)	87 (4)	−5 (9)	824	75	10
H(1C8)	501 (5)	129 (4)	906 (9)	541	55	835
H(2C8)	490 (5)	76 (4)	806 (9)	476	109	803
H(3C8)	558 (4)	66 (4)	895 (8)	537	122	922
H(1C9)	623 (5)	194 (4)	899 (10)	618	206	868
H(2C9)	658 (4)	207 (4)	759 (9)	669	200	734
H(3C9)	679 (5)	146 (4)	841 (9)	666	159	835

Refinements of the $Fe[S_2CN(CH_3)_2]_3$ structure at 25 and 400 K

The coordinates of non-H atoms determined at 295 K were used as initial values in refinement by full-matrix least squares with the structure factors measured at 25 and 400 K. The function minimized was $\sum w(\Delta F)^2$ with weights $w = (\sigma_c^2/4|F_o|^2 + C_1^2|F_o|^2 + C_2)^{-1}$. C_1 and C_2 were adjusted so that constant values of $\langle w(\Delta F)^2 \rangle$ were obtained in different $|F_o|$ and sin θ intervals.

Before the last cycles of refinement of the 25 K structure, all its H atoms (belonging to methyl groups) were located in a difference map. They were included in the refinement with fixed isotropic temperature factors ($B = 1{\cdot}5$ Å²). The final positions were then adjusted to fit a difference map of the 400 K structure from geometrical considerations (tetrahedral methyl C atoms with C—H = 1·0 Å). Four of the six methyl groups were rotated about the C—N bond. The adjusted positions were included in the structure factor calculations for the 400 K structure (fixed coordinates, $B = 8{\cdot}0$ Å²).

Both data sets were tested for isotropic extinction (Zachariasen, 1967). The correction applied to $|F_o|$ differed from 1·00 for *ca* 6% of the reflexions at 400 K. No extinction was detected in the 25 K set.

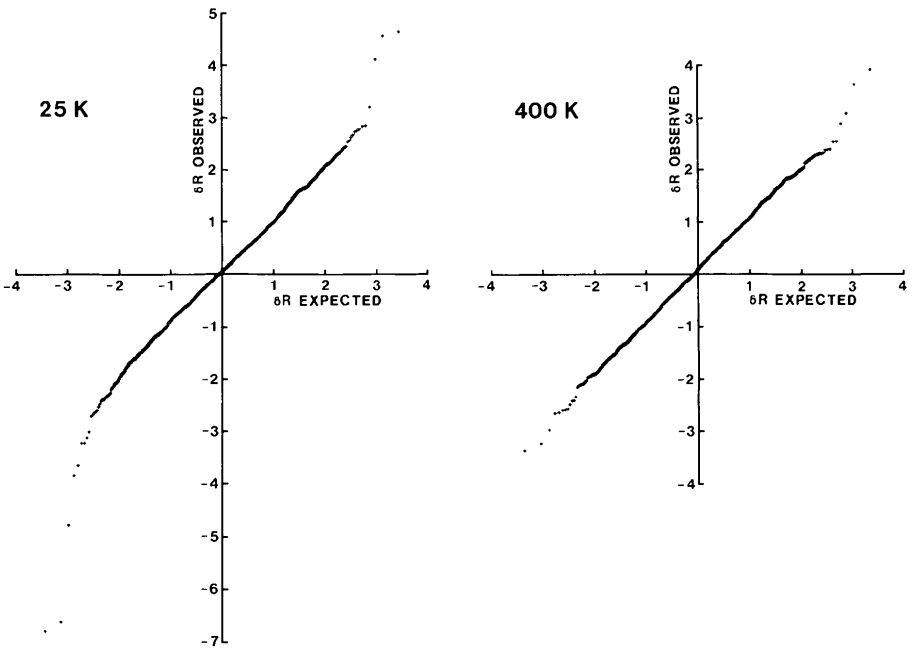

Fig. 2. δR-plot comparison of data and models for $Fe[S_2CN(CH_3)_2]_3$; 25 K: slope 1·012 (4), intercept 0·042 (4); 400 K: slope 0·993 (1), intercept 0·085 (1).

Refinement was terminated when no parameter shift exceeded 5% (25K, 10% for the H parameters) and 1% (400 K) of the corresponding e.s.d. Table 2 gives the positional parameters and approximate isotropic temperature factors at both temperatures.* Data and final models are compared by probability plotting in Fig. 2 where ordered values of $\delta R_t = \Delta F_t/\sigma(|F_o|_t)$ $[\sigma(|F_o|_t) = w^{-1/2}]$ are plotted *vs* those expected for ordered normal deviates (Abrahams & Keve, 1971). Both plots are straight lines with intercepts near zero so the systematic errors appear to be small, even for the 25 K data set in spite of the variation in temperature. The slopes are 1·012 (4) (25 K) and 0·993 (1) (400 K). This (and the related S values of Table 1) indicates that $\sigma(|F_o|)$ is on average correctly estimated.

Scattering factors were taken from *International Tables for X-ray Crystallography* (1974). All factors except those for H were corrected for anomalous dispersion. Since both Mo and Cu $K\alpha$ radiations were used to measure the structure factors at 25 K, the least-squares program was modified to allow the proper correction of each $|F_c|$.

* Lists of structure factors and anisotropic thermal parameters (the non-H atoms are assumed to vibrate within the simple harmonic approximation at both temperatures) have been deposited with the British Library Lending Division as Supplementary Publication No. SUP 35596 (16 pp.). Copies may be obtained through The Executive Secretary, International Union of Crystallography, 5 Abbey Square, Chester CH1 2HU, England.

Description of the $Fe[S_2CN(CH_3)_2]_3$ structure at 25 and 400 K

The general features of the structure of tris(*N*,*N*-dimethyldithiocarbamato)iron(III) are the same at 25 and 400 K. Fig. 3 shows stereoscopic pairs of drawings of the mononuclear complex at the two temperatures. Tables 3 and 4 give selected interatomic distances,

Table 3. *Interatomic distances* (Å) *in the* FeS_6 *polyhedron of* $Fe[S_2CN(CH_3)_2]_3$

	25 K	400 K
Fe–S(1)	2·294 (4)	2·407 (3)
Fe–S(2)	2·312 (4)	2·420 (3)
Fe–S(3)	2·306 (4)	2·414 (3)
Fe–S(4)	2·308 (4)	2·430 (3)
Fe–S(5)	2·293 (3)	2·403 (3)
Fe–S(6)	2·305 (3)	2·418 (3)
S(1)–S(2)	2·831 (4)	2·866 (4)
S(3)–S(4)	2·827 (4)	2·888 (4)
S(5)–S(6)	2·824 (5)	2·880 (4)
S(1)–S(3)	3·299 (8)	3·479 (4)
S(1)–S(6)	3·440 (5)	3·644 (4)
S(3)–S(6)	3·377 (6)	3·572 (4)
S(2)–S(4)	3·386 (8)	3·568 (4)
S(2)–S(5)	3·401 (6)	3·589 (4)
S(4)–S(5)	3·283 (5)	3·446 (4)
S(1)–S(4)	3·476 (9)	3·708 (4)
S(3)–S(5)	3·492 (4)	3·710 (4)
S(6)–S(2)	3·510 (4)	3·733 (4)

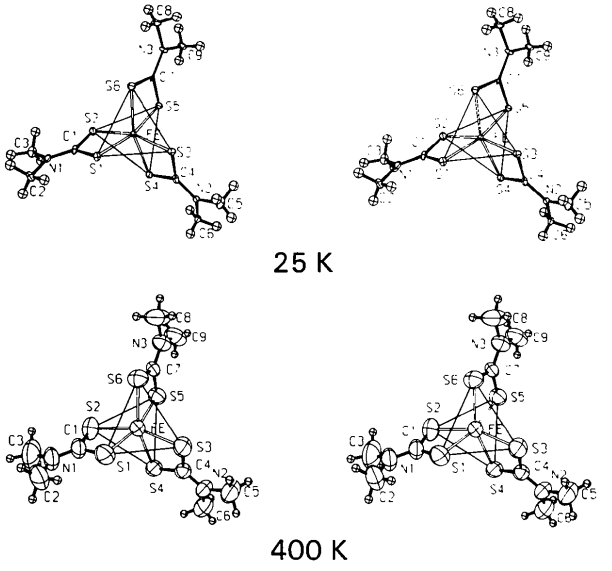

Fig. 3. Stereoscopic drawings of $Fe[S_2CN(CH_3)_2]_3$ at 25 and 400 K viewed along the pseudo threefold axis (the complex has approximately D_3 symmetry). The thermal ellipsoids of the atoms are scaled to include 50% probability except for the H atoms at 400 K which are drawn as spheres with radii of 0·1 Å.

angles and torsion angles in the FeS_6 core and the ligands. The mean observed Fe–S distance increases from 2·302 (3) Å in the low-spin complex at 25 K to 2·415 (4) Å in the high-spin complex at 400 K.

There are only van der Waals forces between the complexes. Fig. 4 shows the resulting packing arrangement. There are interactions both between the planar ligands No. 1 and 2 of different complexes, along lines parallel to x, and between methyl groups about planes parallel to $2x - y = 0$. There is a slight change in the relative orientation of the complexes when the temperature increases from 25 to 400 K. The closest contacts are across the centres of symmetry with Fe–Fe = 6·132 (1) at 25 and 6·511 (1) Å at 400 K, concurrent with an increase in the molecular volume of the complex from 431 (4) to 467 (1) Å^3, which thus reflects both the changing size of the FeS_6 core when the spin state changes, but also a more efficient crystal packing at 25 than at 400 K made possible by the very small vibration amplitudes. The magnitudes of the β_{ij} values at 25 K are at most only a few times their e.s.d.'s and for C(7) less than 1σ. The r.m.s. thermal displacements increase from an average of 0·12 (2) Å at 25 K to an average of 0·29 (5) Å at 400 K. At a slightly higher temperature, about 425 K, the crystals sublime when the intermolecular interactions are balanced by the thermal energy of the complex.

The changes in bond distances and angles in the ligands are very small between the two temperatures. The only appreciable difference is in the S–C–S angles: their mean value increases from 110·6 (1) to 114·7 (4)°. Probability plotting of interatomic distances between the non-H ligand atoms (Albertsson, Elding & Oskarsson, 1979) indicates that their pooled e.s.d.'s are correctly estimated as could be expected from the δR plots of Fig. 2. There is a small but

Table 4. *Bond distances, bond angles and torsion angles in the three ligands of* $Fe[S_2CN(CH_3)_2]_3$ (Å *and* deg) *and r.m.s. deviation* (Å) *from the least-squares planes through the* S_2CNC_2 *groups*

	25 K	400 K
(*a*) Ligand 1		
S(1)–C(1)	1·724 (7)	1·715 (12)
S(2)–C(1)	1·716 (8)	1·701 (12)
C(1)–N(1)	1·301 (10)	1·303 (15)
N(1)–C(2)	1·468 (11)	1·449 (20)
N(1)–C(3)	1·467 (10)	1·420 (22)
S(1)–C(1)–S(2)	110·8 (4)	114·1 (6)
S(1)–C(1)–N(1)	124·5 (6)	122·5 (9)
S(2)–C(1)–N(1)	124·7 (5)	123·4 (9)
C(1)–N(1)–C(2)	123·1 (6)	123·0 (1·2)
C(1)–N(1)–C(3)	121·4 (7)	123·0 (1·2)
C(2)–N(1)–C(3)	115·5 (7)	114·0 (1·2)
S(1)–C(1)–N(1)–C(2)	−0·7 (1·0)	−0·9 (1·7)
S(1)–C(1)–N(1)–C(3)	179·8 (6)	−179·5 (1·1)
S(2)–C(1)–N(1)–C(3)	−0·3 (1·0)	1·7 (1·8)
S(2)–C(1)–N(1)–C(2)	179·2 (6)	−179·7 (1·0)
R.m.s. deviation	0·0022	0·0021
(*b*) Ligand 2		
S(3)–C(4)	1·713 (7)	1·707 (10)
S(4)–C(4)	1·724 (7)	1·727 (10)
C(4)–N(2)	1·313 (9)	1·307 (12)
N(2)–C(5)	1·466 (10)	1·455 (14)
N(2)–C(6)	1·459 (11)	1·438 (14)
S(3)–C(4)–S(4)	110·7 (4)	114·5 (5)
S(3)–C(4)–N(2)	125·6 (5)	124·2 (7)
S(4)–C(4)–N(2)	123·7 (5)	121·3 (7)
C(4)–N(2)–C(5)	121·4 (6)	120·9 (9)
C(4)–N(2)–C(6)	122·5 (6)	123·0 (8)
C(5)–N(2)–C(6)	116·1 (6)	116·1 (8)
S(3)–C(4)–N(2)–C(5)	2·0 (1·0)	2·0 (1·4)
S(3)–C(4)–N(2)–C(6)	−179·1 (6)	−179·2 (8)
S(4)–C(4)–N(2)–C(6)	−0·1 (1·0)	−1·6 (1·4)
S(4)–C(4)–N(2)–C(5)	−179·0 (6)	179·6 (8)
R.m.s. deviation	0·0040	0·0032
(*c*) Ligand 3		
S(5)–C(7)	1·716 (8)	1·699 (10)
S(6)–C(7)	1·723 (8)	1·707 (10)
C(7)–N(3)	1·328 (12)	1·302 (14)
N(3)–C(8)	1·449 (11)	1·464 (16)
N(3)–C(9)	1·461 (10)	1·446 (16)
S(5)–C(7)–S(6)	110·4 (5)	115·5 (6)
S(5)–C(7)–N(3)	124·6 (5)	121·6 (7)
S(6)–C(7)–N(3)	124·9 (6)	122·9 (8)
C(7)–N(3)–C(8)	123·0 (6)	121·7 (9)
C(7)–N(3)–C(9)	120·7 (6)	123·3 (9)
C(8)–N(3)–C(9)	116·4 (7)	115·0 (9)
S(6)–C(7)–N(3)–C(8)	−5·8 (1·1)	−4·4 (1·4)
S(6)–C(7)–N(3)–C(9)	174·2 (6)	174·4 (8)
S(5)–C(7)–N(3)–C(9)	−3·4 (1·0)	−3·1 (1·4)
S(5)–C(7)–N(3)–C(8)	176·5 (6)	178·1 (8)
R.m.s. deviation	0·0202	0·0160

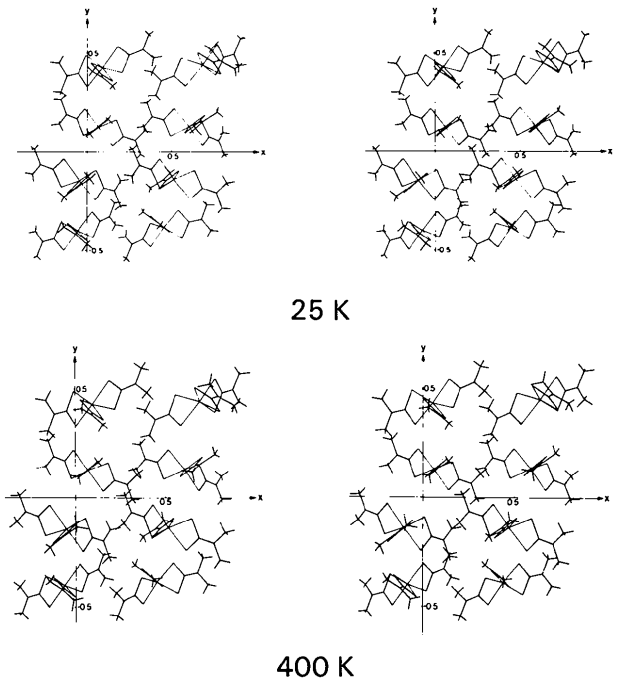

Fig. 4. Stereoscopic drawings of the crystal packing of $Fe[S_2CN(CH_3)_2]_3$ at 25 and 400 K.

Table 5. *The geometry of the coordination polyhedron of* $Fe[S_2CN(CH_3)_2]_3$ *at* 25, 150, 295 *and* 400 K

Temperature (K)	25	150	295	400
μ_{eff}	–	2·40	4·03	4·83
Fe–S (Å)	2·302 (3)	2·339 (3)	2·396 (5)	2·415 (4)
δ(Fe–S) (Å)	–	0·036 (1)	0·093 (3)	0·114 (2)
Δ (Å)	0·191	0·218	0·248	0·269
Ligand bite (S–S) (Å)	2·827 (2)	2·843 (3)	2·872 (4)	2·878 (6)
Edge of triangular face (Å)	3·364 (25)	3·424 (27)	3·517 (30)	3·550 (30)
Height of prism (Å)	2·474 (4)	2·498 (3)	2·542 (3)	2·554 (4)
Torsion angle (°)	41 (1)	40 (1)	39 (1)	39 (2)
Tilt angle between triangular faces (°)	1·6 (6)	1·8 (8)	1·9 (1·0)	2·0 (1·0)
Fe – centroid of prism (Å)	0·027 (3)	0·033 (2)	0·039 (2)	0·036 (2)

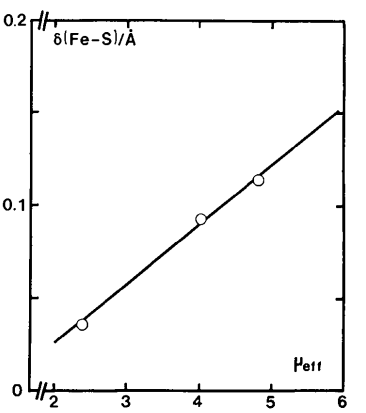

Fig. 5. The mean observed increase in Fe–S [δ(Fe–S)] between 25 K and T, as a function of $\mu_{eff}(T)$.

significant decrease in the apparent bond lengths when the temperature increases. The average decrease is 0·011 (3) Å between 25 and 400 K.

The non-H atoms of ligands No. 1 and 2 are planar as shown by both the torsion angles and the r.m.s. deviations from the least-squares planes through the atoms (Table 4). Ligand No. 3 is slightly non-planar at both temperatures. This is most probably caused by the intermolecular packing forces.

Discussion

Table 5 gives the geometrical characteristics of the FeS_6 polyhedron in $Fe[S_2CN(CH_3)_2]_3$ at 25, 150, 295 and 400 K. The values at 150 and 295 K are taken from Albertsson & Oskarsson (1977). The mean observed increase in Fe–S from its length at 25 K [denoted δ(Fe–S)] is plotted *vs* μ_{eff} in Fig. 5. Linear extrapolation to the spin-only high-spin value of Fe^{III}, $\mu_{eff} = 5{\cdot}92$, gives the difference 0·15 Å between the high- and low-spin radii of Fe^{3+}. This difference is much larger than the 0·10 Å given by Shannon (1976) in his tabulation of ionic radii, but it is in agreement with the Fe–S distance of 2·443 Å in high-spin $Fe(S_2CNC_4H_8O)_3.H_2O$ (Butcher & Sinn, 1976) and the 2·306 and 2·297 Å in respectively low-spin $Fe[S_2CN(C_2H_5)_2]_3$ (Leipoldt & Coppens, 1973) and low-spin $Fe(S_2CNC_4H_4)_3.0{\cdot}5CH_2Cl_2$ (Bereman, Churchill & Nalewajek, 1979).

To obtain a single measure of the distortion of the FeS_6 polyhedron at the various temperatures, we have calculated the r.m.s. separation Δ after a best molecular fit of the FeS_6 coordinates to those of the ideal octahedron (Dollase, 1974; Albertsson, Elding & Oskarsson, 1979). At each temperature the mean observed Fe–S distance was normalized to 1 Å. The least distorted polyhedron is the one at 25 K. When the temperature increases, the Fe–S length and the ligand bite (S–S) increase causing an increase in the height of the polyhedron. The ratio (S–S)/(Fe–S) decreases from 1·228 at 25 to 1·191 at 400 K. Simple electrostatic calculations of ligand–ligand repulsions and the trigonal twist (torsion) made according to Avdeef & Fackler (1975) predict a decrease in the torsion angle from 41° at 25 K to 36° at 400 K. The observed angles have values in this interval but the decrease is not significant.

A ^{13}C NMR study by Gregson & Doddrell (1975) indicates that the metal–ligand π-bonding increases when μ_{eff} decreases. If there is an accompanying change in the ligand S–C and C–N lengths it is on a scale below what can be detected from crystal structure determinations by X-ray diffraction methods. We have recorded ESCA electron spectra of the non-H atoms in $Fe[S_2CN(CH_3)_2]_3$ at 150, 200, 250 and 300 K. The

spectra revealed an increase of the charges on Fe, S and N with decreasing temperature: about 0·05–0·1 a.u. in the interval 300–150 K. There are two types of C atoms in the ligand resulting in broad spectra in which no changes in binding energy could be detected. The ESCA study indicates that in the low-spin complex electron density is moved from the Fe, S and N atoms most probably into the Fe–S region resulting in a shorter and stronger Fe–S bond than in the high-spin complex.

We thank Dr B. Folkesson for measuring the ESCA electron spectra and for many helpful discussions, and Ms L. Timby for computing and drawing the illustrations and for help with part of the experimental work. The Swedish Natural Science Research Council gave financial support, which is gratefully acknowledged.

References

ABRAHAMS, S. C. & KEVE, E. T. (1971). *Acta Cryst.* A**27**, 157–165.

ALBERTSSON, J., ELDING, I. & OSKARSSON, Å. (1979). *Acta Chem. Scand. Ser. A*, **33**, 703–717.

ALBERTSSON, J. & OSKARSSON, Å. (1977). *Acta Cryst.* B**33**, 1871–1877.

ALBERTSSON, J., OSKARSSON, Å. & STÅHL, K. (1979). *J. Appl. Cryst.* **12**, 537–544.

AVDEEF, A. & FACKLER, J. P. JR (1975). *Inorg. Chem.* **14**, 2002–2006.

BEREMAN, R. D., CHURCHILL, M. R. & NALEWAJEK, D. (1979). *Inorg. Chem.* **18**, 3112–3117.

BUTCHER, R. J. & SINN, E. (1976). *J. Am. Chem. Soc.* **98**, 5159–5168.

DOLLASE, W. A. (1974). *Acta Cryst.* A**30**, 513–517.

EWALD, A. H., MARTIN, R. L., SINN, E. & WHITE, A. H. (1969). *Inorg. Chem.* **8**, 1837–1846.

FOLKESSON, B. (1973). *Acta Chem. Scand.* **27**, 287–302.

GREGSON, K. & DODDRELL, D. M. (1975). *Chem. Phys. Lett.* **31**, 125–128.

International Tables for X-ray Crystallography (1974). Vol. IV. Birmingham: Kynoch Press.

LEHMANN, M. S. & LARSEN, F. K. (1974). *Acta Cryst.* A**30**, 580–584.

LEIPOLDT, J. G. & COPPENS, P. (1973). *Inorg. Chem.* **12**, 2269–2274.

LISSALDE, F., ABRAHAMS, S. C. & BERNSTEIN, J. L. (1978). *J. Appl. Cryst.* **11**, 31–34.

SHANNON, R. D. (1976). *Acta Cryst.* A**32**, 751–767.

WHITE, A. H., ROPER, R., KOKOT, E., WATERMAN, H. & MARTIN, R. L. (1964). *Aust. J. Chem.* **17**, 294–313.

ZACHARIASEN, W. H. (1967). *Acta Cryst.* **23**, 558–564.

Acta Cryst. (1981). B**37**, 56–61

Structure du μ-Oxo-bis[dioxo(*o*-phénanthroline-*N*,*N'*)-(thiocyanato-*N*)molybdène(VI)]–Acétone

PAR BERNARD VIOSSAT

Laboratoire de Chimie Minérale, UER de Médecine et de Pharmacie, 34 *rue du Jardin des Plantes,* 86034 *Poitiers CEDEX, France*

ET NOËL RODIER

Laboratoire de Chimie Minérale, Faculté des Sciences Pharmaceutiques et Biologiques, rue J.-B. Clément, 92290 *Châtenay-Malabry, France*

(*Reçu le* 28 *janvier* 1980, *accepté le* 16 *septembre* 1980)

Abstract

The crystal structure of $[Mo_2(C_{12}H_8N_2)_2(NCS)_2O_5].C_3H_6O$ was solved by Patterson and Fourier techniques and refined by full-matrix least-squares methods to a final $R = 0{\cdot}036$ for 2907 independent reflections. The space group is $P2_1/b$ and the unit-cell dimensions are: $a = 8{\cdot}81\ (1)$, $b = 18{\cdot}64\ (2)$, $c = 20{\cdot}27\ (2)$ Å, $\gamma = 106{\cdot}58\ (8)°$, with $Z = 4$, $D_c = 1{\cdot}70\ (2)$, $D_m = 1{\cdot}679$ Mg m^{-3}. The H atoms of the phenanthroline groups were included in structure factor calculations but not refined. Those of the acetone molecule were not searched for. $[Mo_2(C_{12}H_8N_2)_2(NCS)_2O_5]$ is a binuclear, oxo-bridged complex of Mo^{VI}. Each Mo atom has a distorted octahedron of three N and three O atoms. Of the three N atoms, two belong to a phenanthroline and one to a NCS ligand. The Mo–O–Mo' bridge is bent. The complex molecule shows a non-negligible torsion around the Mo–Mo' axis, but the two chelating phenanthroline

0567-7408/81/010056-06$01.00